Supplementary

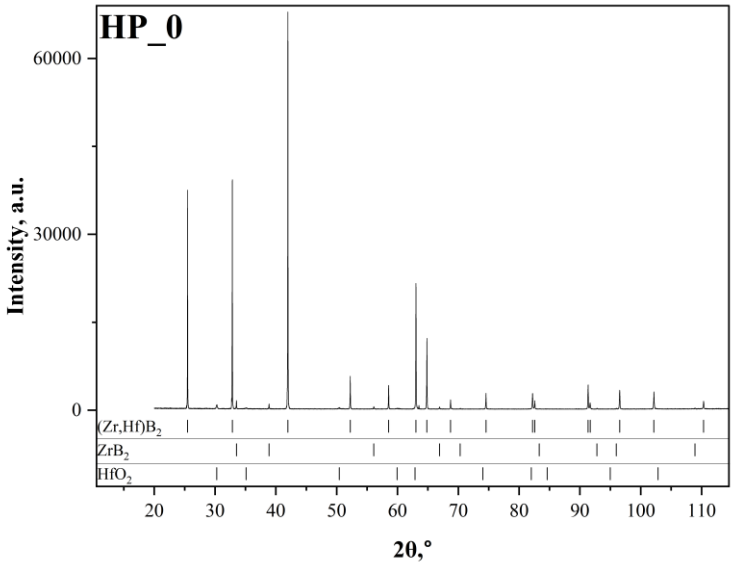
Modification of Thermo-Chemical Properties of Hot-Pressed ZrB_2-HfB_2 Composites by Incorporation of Carbides (SiC, B_4C, WC) or Silicides ($MoSi_2$, $CrSi_2$) Additive

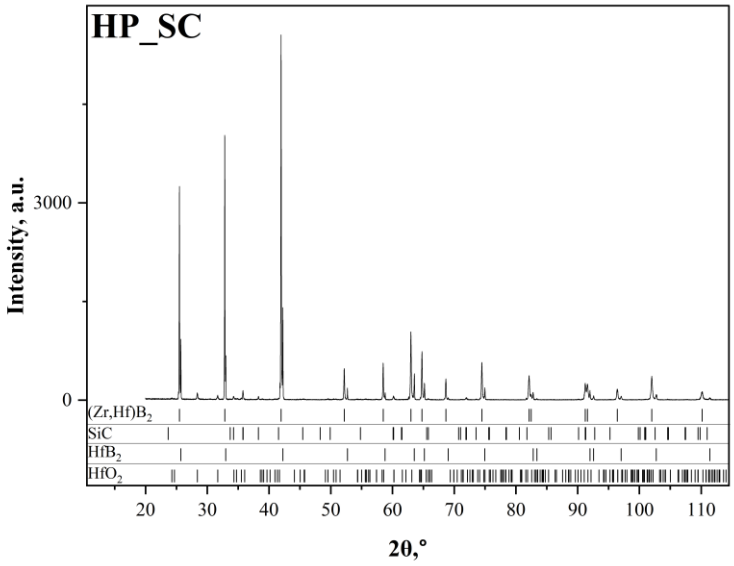
Agnieszka Gubernat [1], Kamil Kornaus [1], Dariusz Zientara [1], Łukasz Zych [1], Paweł Rutkowski [1], Sebastian Komarek [1], Annamaria Naughton-Duszova [2], Yongsheng Liu [3], Leszek Chlubny [1], Zbigniew Pędzich [1*]

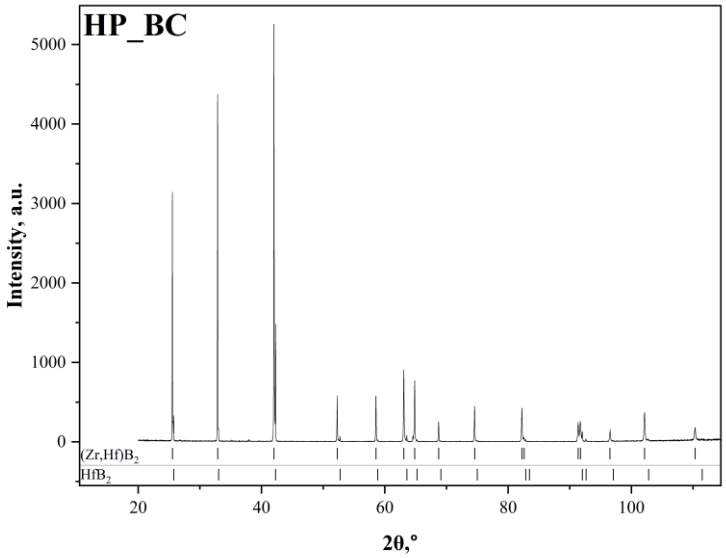
[1] Faculty of Materials Science and Ceramics, AGH University of Krakow, al. Adama Mickiewicza 30, 30-059 Kraków, Poland; gubernat@agh.edu.pl (A.G.); kornaus@agh.edu.pl (K.K.); zientara@agh.edu.pl (D.Z.); lzych@agh.edu.pl (Ł.Z.); pawelr@agh.edu.pl (P.R.); seko@agh.edu.pl (S.K.); leszek@agh.edu.pl (L.C.)
[2] Institute of Materials Research, Slovak Academy of Sciences, 47 Watsonova St., 040 01 Košice, Slovakia; aduszova@saske.sk
[3] Science and Technology on Thermostructural Composite Materials Laboratory, Northwestern Polytechnical University, Xi'an 710072, China; yongshengliu@nwpu.edu.cn
* Correspondence: pedzich@agh.edu.pl; Tel.: +48-12-617-23-97

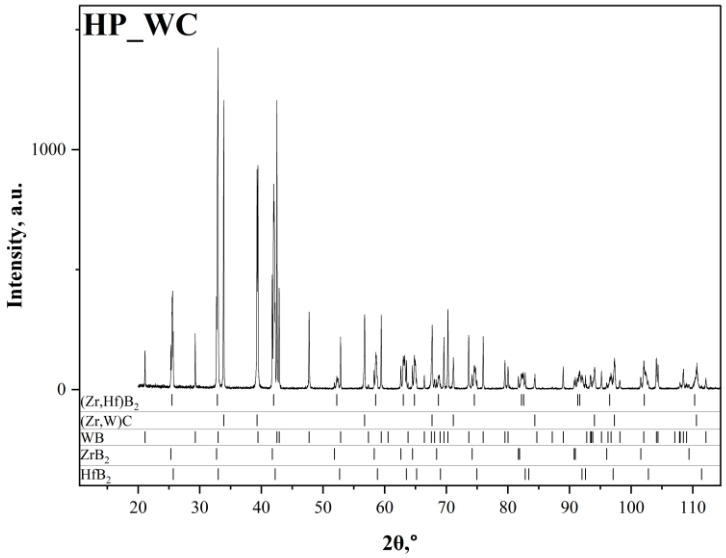
Supplementary Materials

Figure S1 shows XRD patterns of all composites.




HP_SC
Intensity, a.u.
3000
0
(Zr,Hf)B2
SiC
HfB2
HfO2
20
30
40
50
60
70
80
90
100
110
2θ,°


HP_BC
Intensity, a.u.
5000
4000
3000
2000
1000
0
(Zr,Hf)B2
HfB2
20
40
60
80
100
2θ,°


HP_WC
Intensity, a.u.
1000
0
(Zr,Hf)B2
(Zr,W)C
WB
ZrB2
HfB2
20
30
40
50
60
70
80
90
100
110
2θ,°

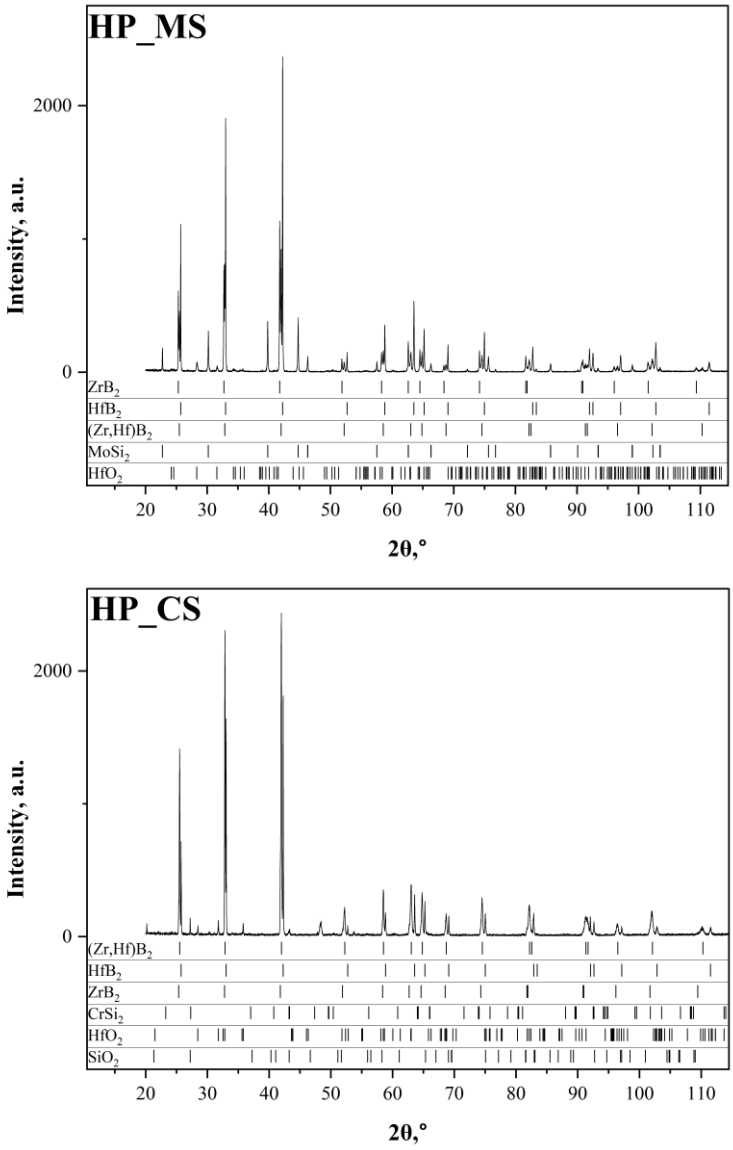


Figure S1. XRD patterns of ZrB_2-HfB_2-MX composites.

Figure S2 shows an SEM image of the HP_BC composite together with an EDS analysis of the chemical composition in the micro-areas. The analysis shows that the darkest areas visible in the micrograph are composed of boron and carbon.

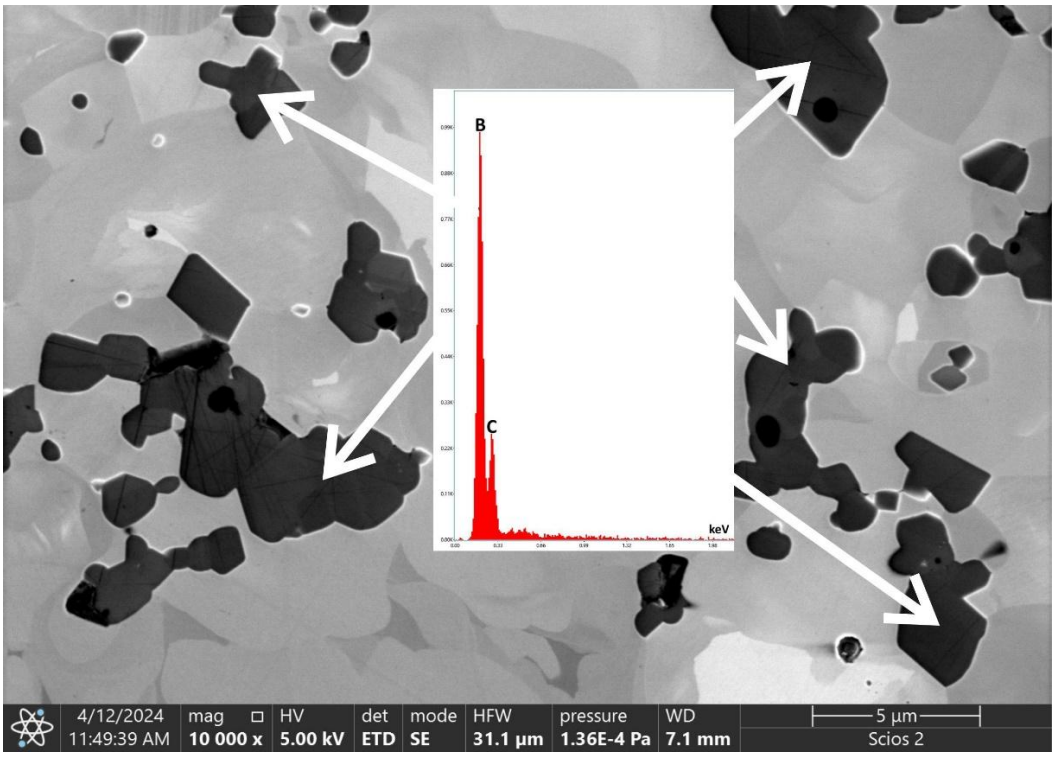


Figure S2. SEM microstructure and spot EDS chemical analysis of the HP_BC composite.

Figure S3 presents the results of the XRD phase composition analysis of the HP_BC composite performed using the method with an internal standard. Zinc oxide ZnO in an amount of approximately 15 % was used as the standard. The results of the analysis show that significant amounts of amorphous phase are present in the HP_BC composite. This phase is observed in the SEM images as the darkest boron-rich areas. The roentgenogram shows impurities in the form of SiO_2 and Al_2O_3, which originate from the mortar in which the sample was crushed.

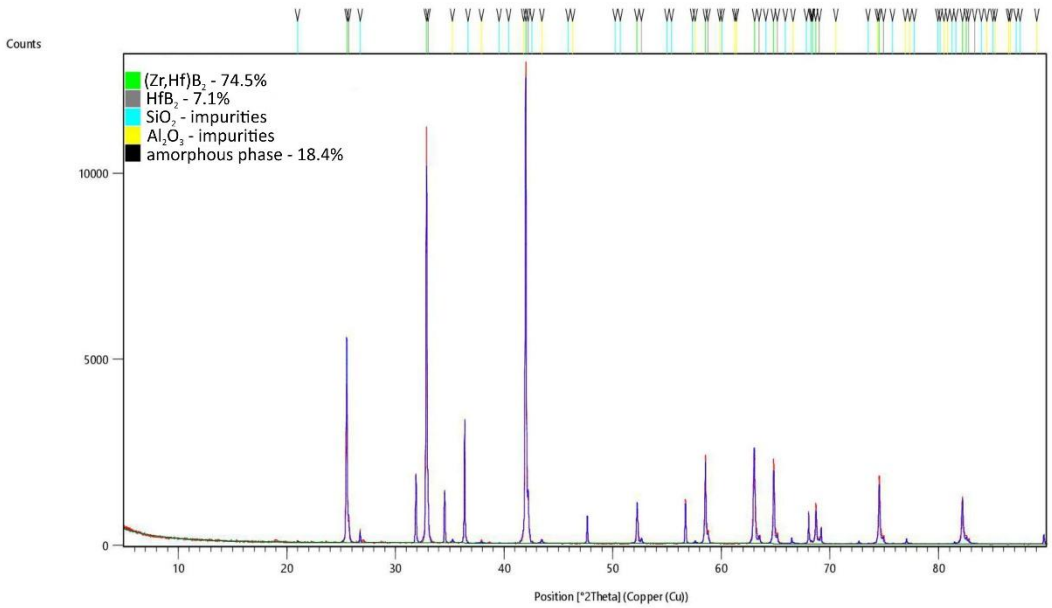


Figure S3. Results of qualitative and quantitative analysis of the phase composition of the HP_BC composite with ZnO standard.

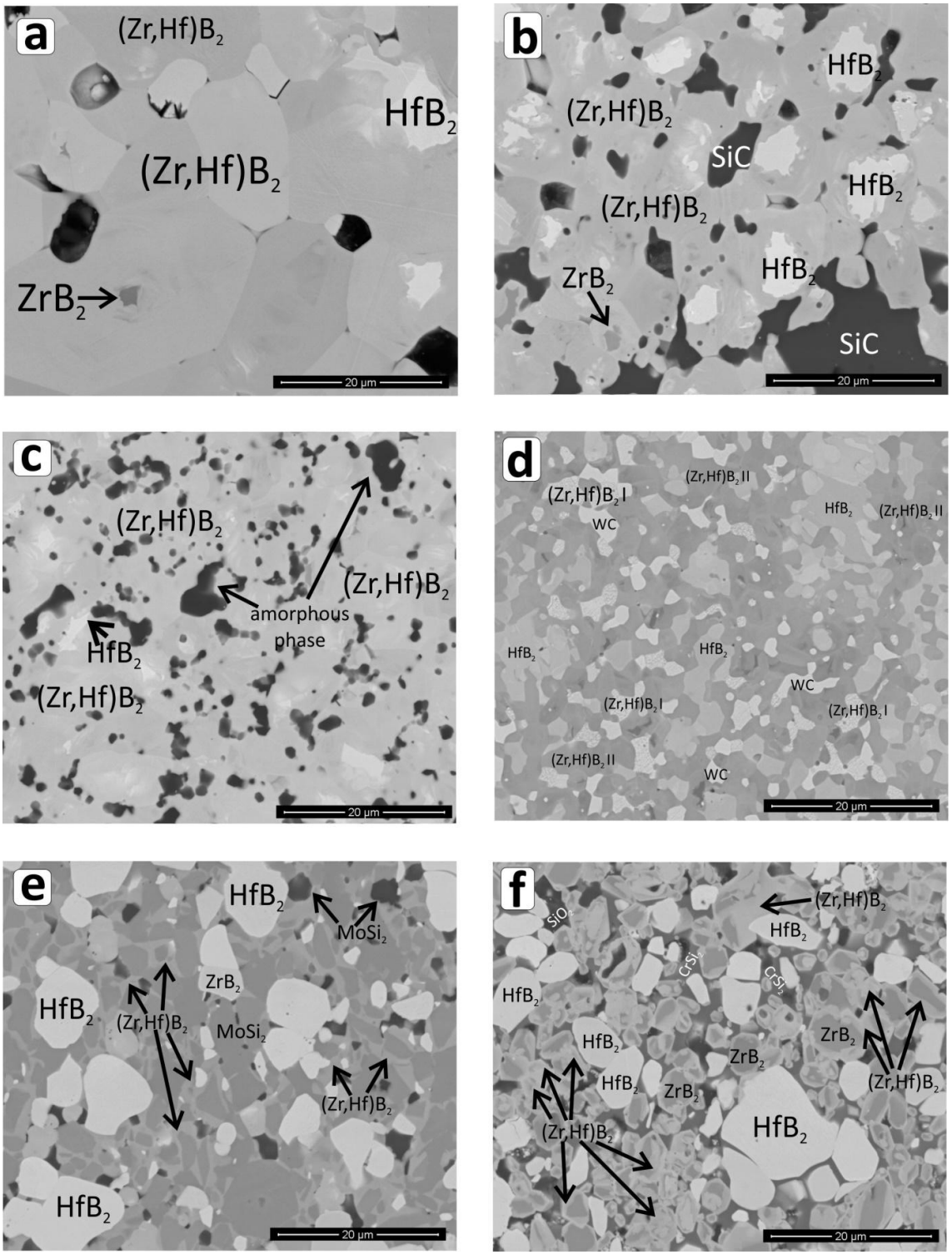


Figure S4. SEM microstructures of ZrB_2-HfB_2 composites sintered by HP: a) without additives, b) with SiC, c) with B_4C, d) with WC, e) with $MoSi_2$ f) with $CrSi_2$ additives.

The cross-sections of the oxidated samples at 1400°C are showed in Figure S5.

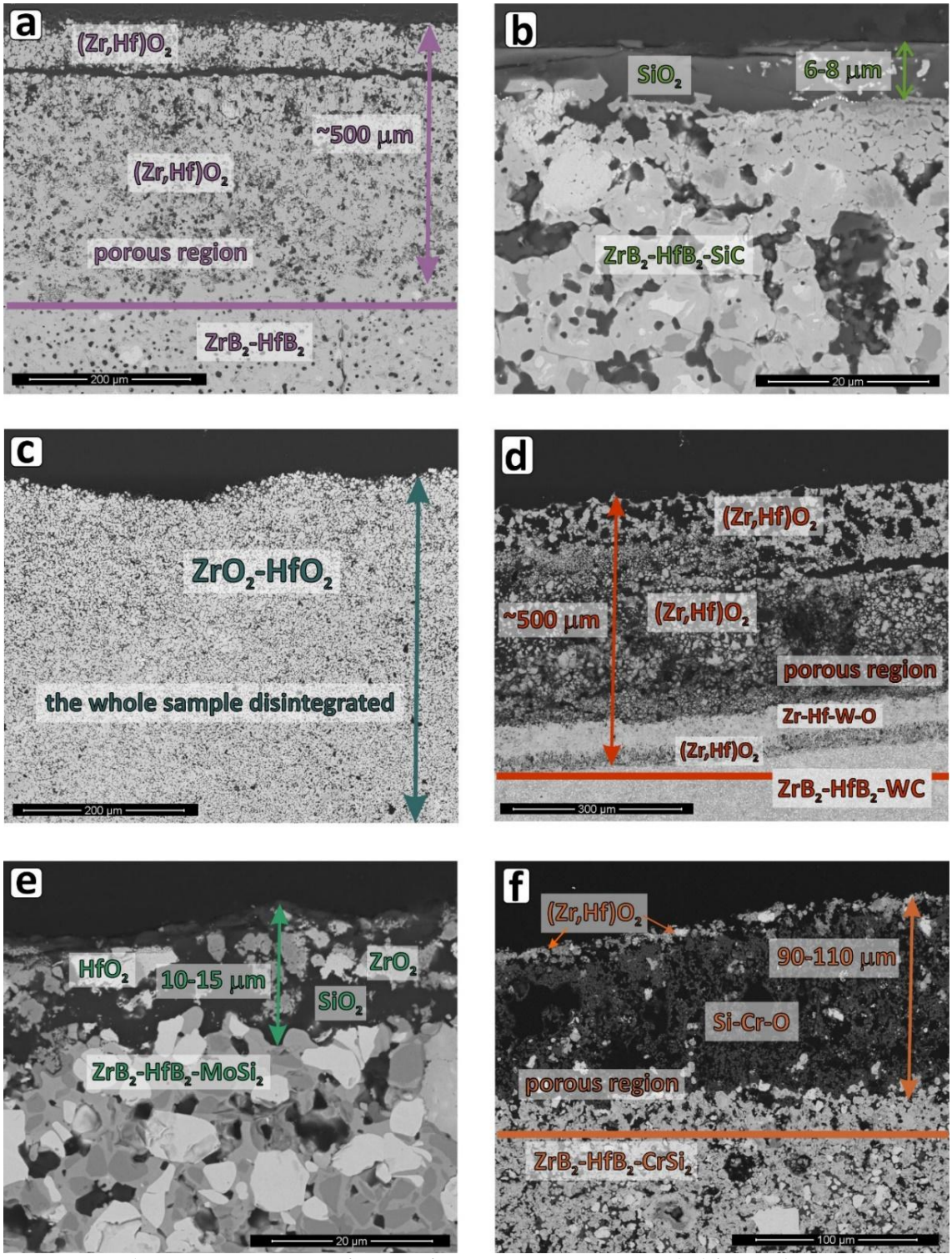


Figure S5. Oxidation cross sections of ZrB_2-HfB_2-MX composites recorded for oxidation temperature 1400 °C: a) HP_0, b) HP_SC; c) HP_BC; d) HP_WC; e) HP_MS i f) HP_CS.

The following **Figures S6 – S11** show elemental distribution maps along the oxidation profiles of all the composites tested.

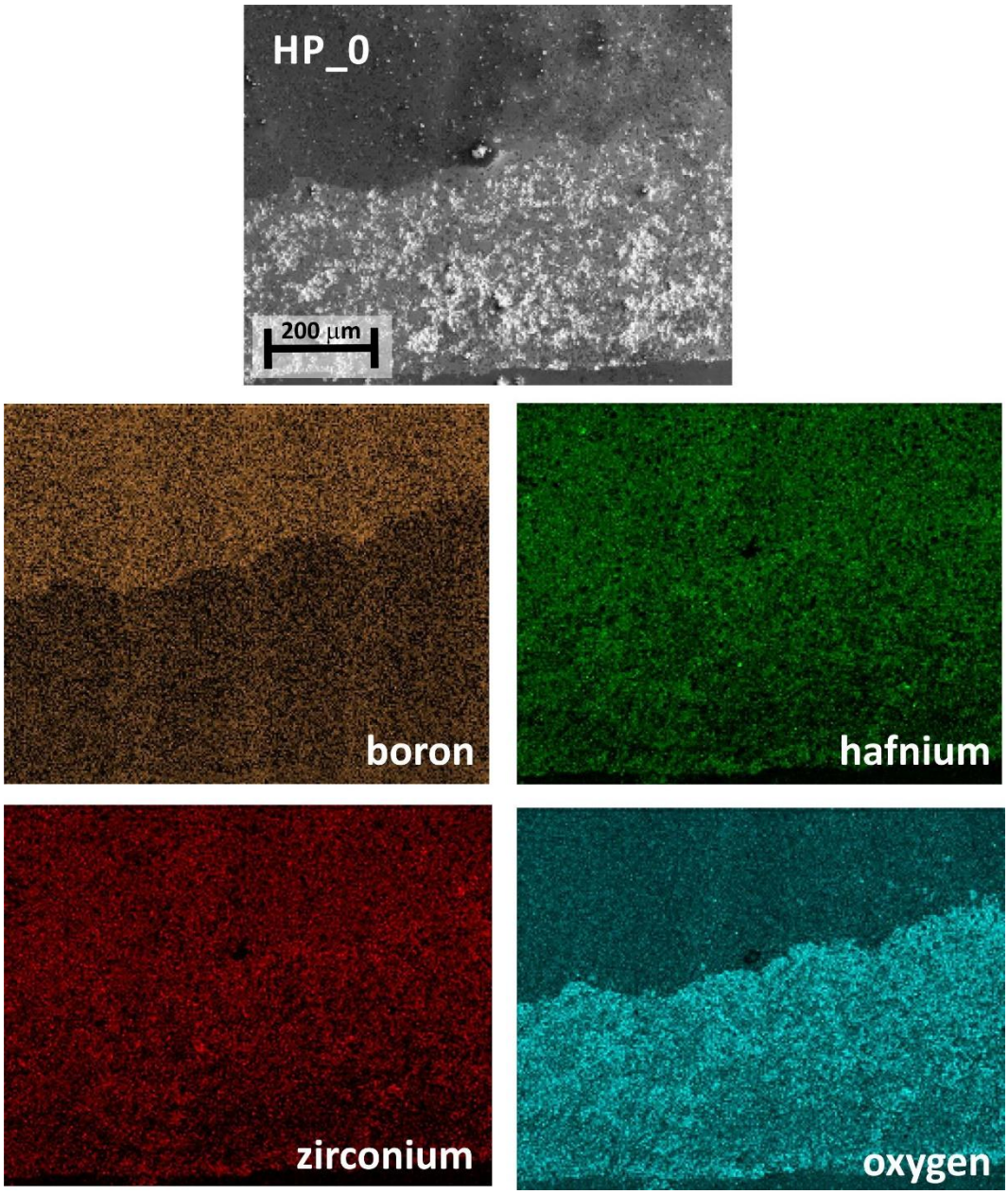


Figure S6. Elemental distribution maps along the oxidation profile in HP_0 composite.

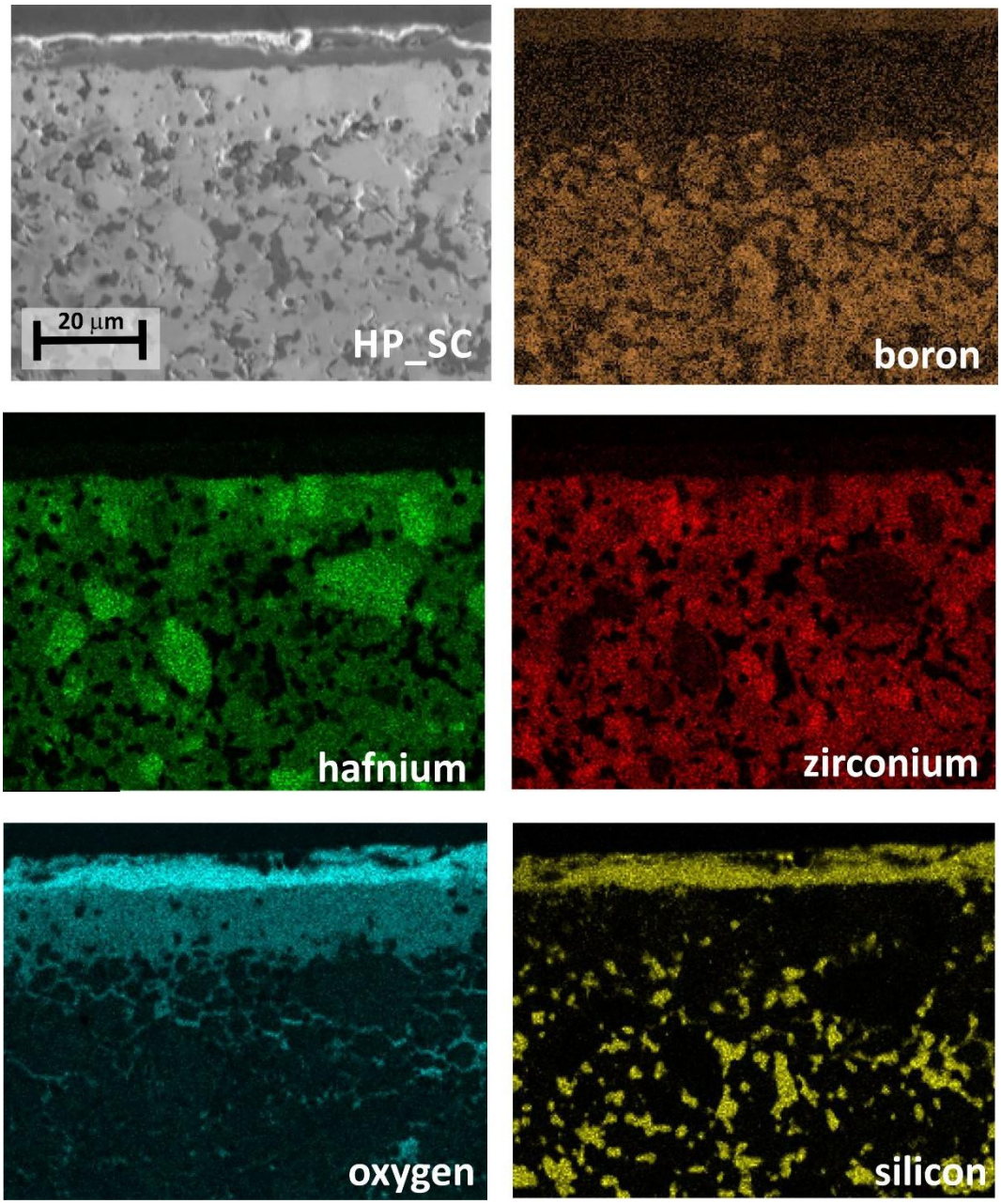


Figure S7. Elemental distribution maps along the oxidation profile in the HP_SC composite.

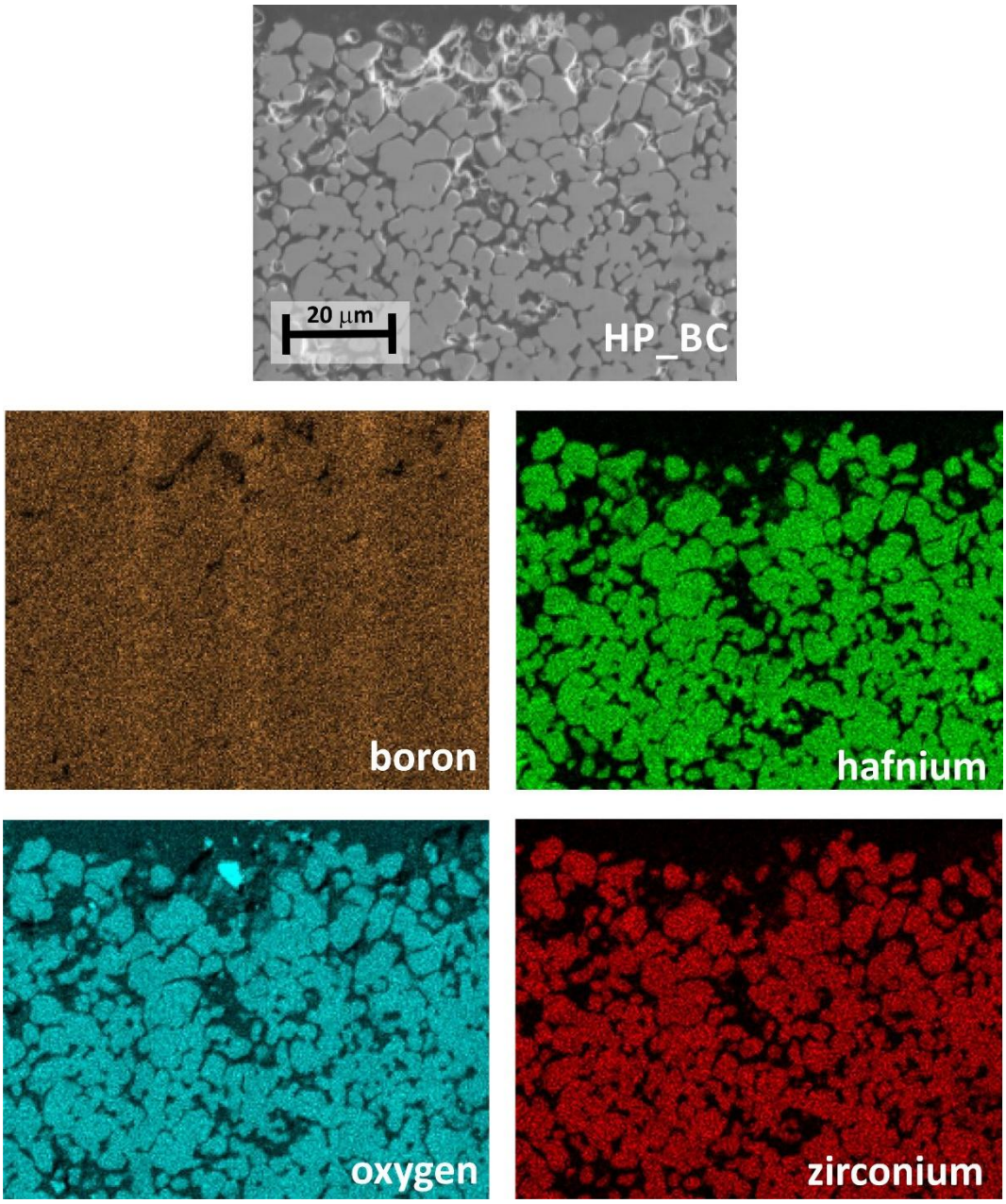


Figure S8. Elemental distribution maps along the oxidation profile in the HP_BC composite.

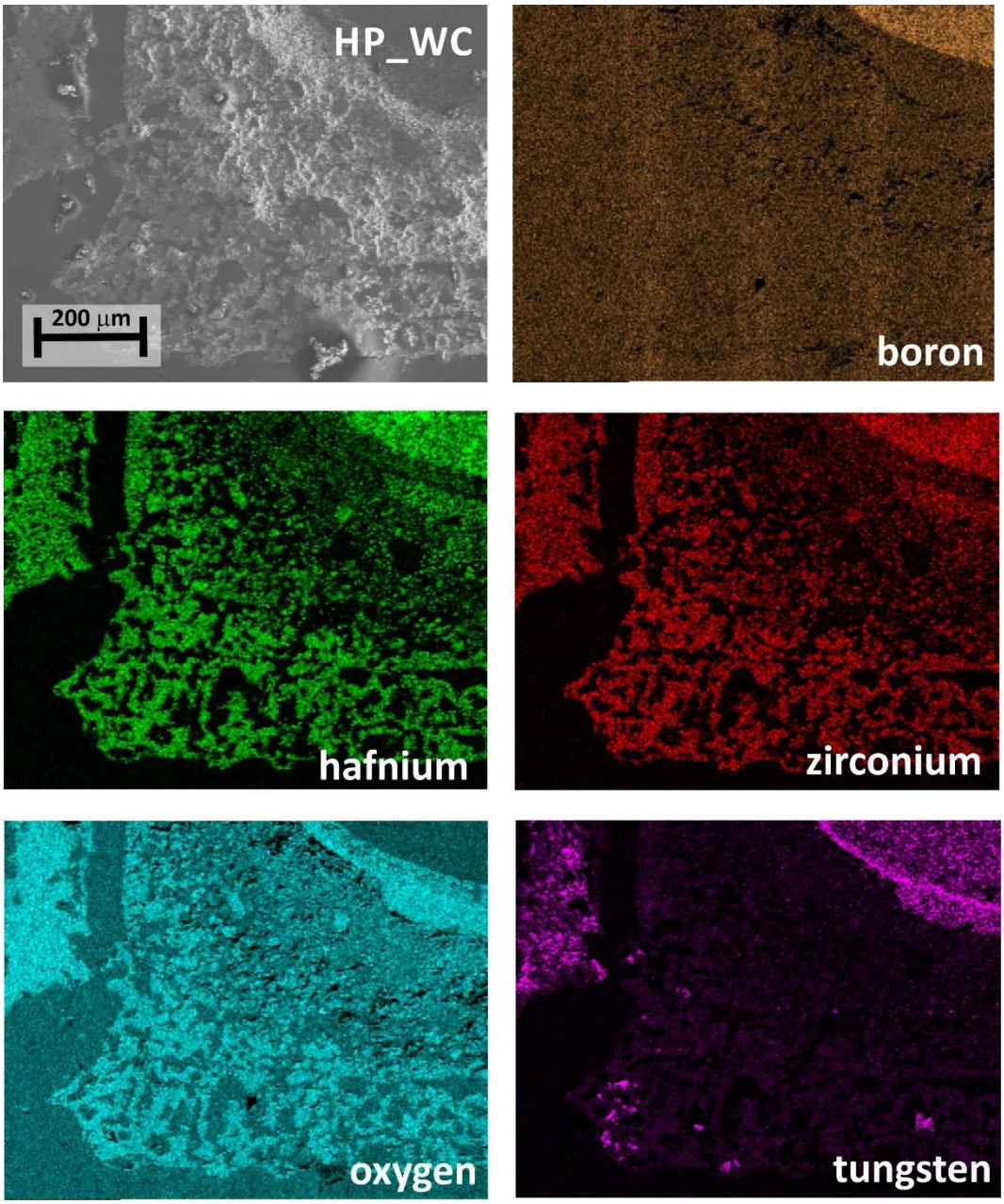


Figure S9. Elemental distribution maps along the oxidation profile in HP_WC composite.

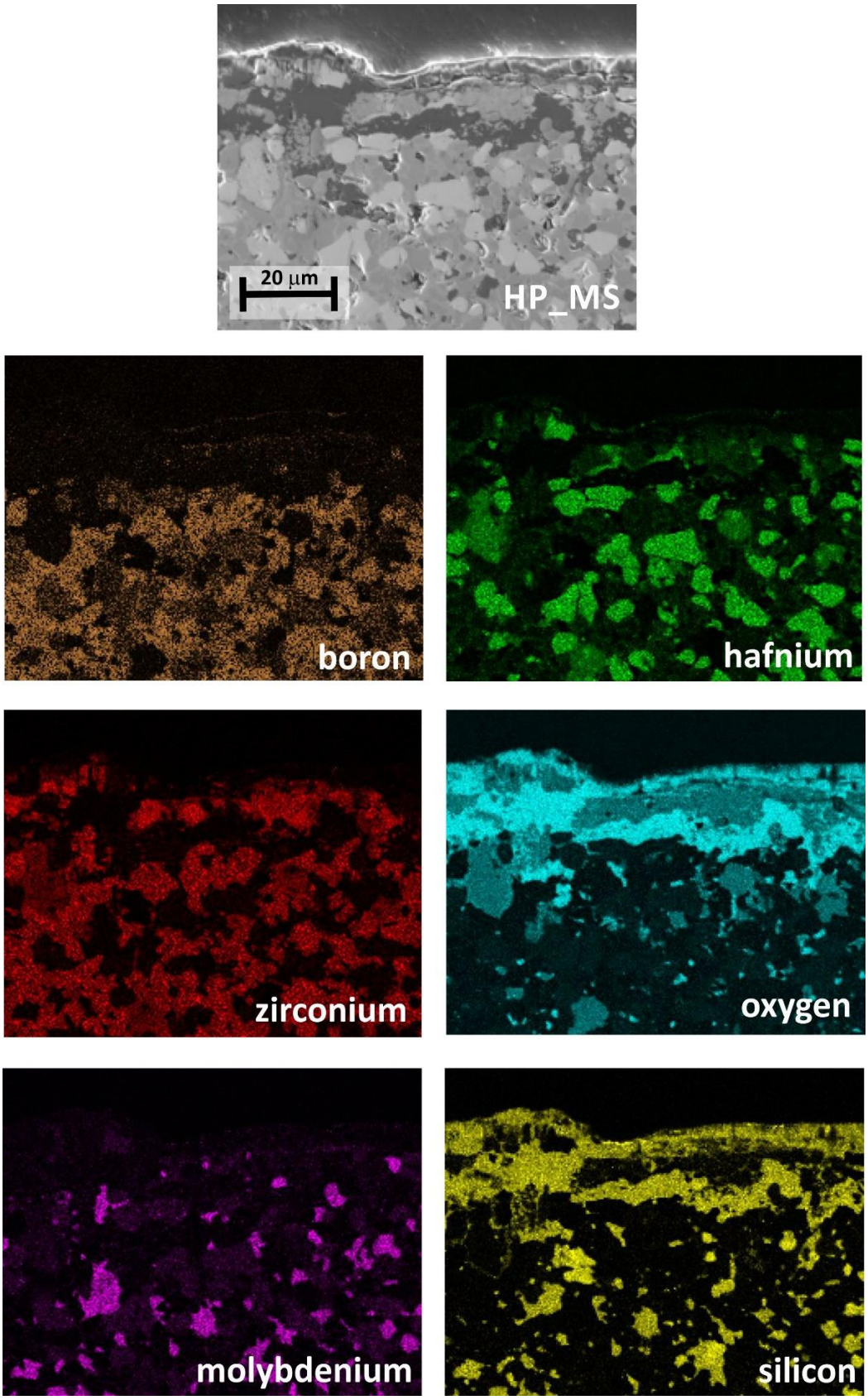


Figure S10. Elemental distribution maps along the oxidation profile in the HP_MS composite.

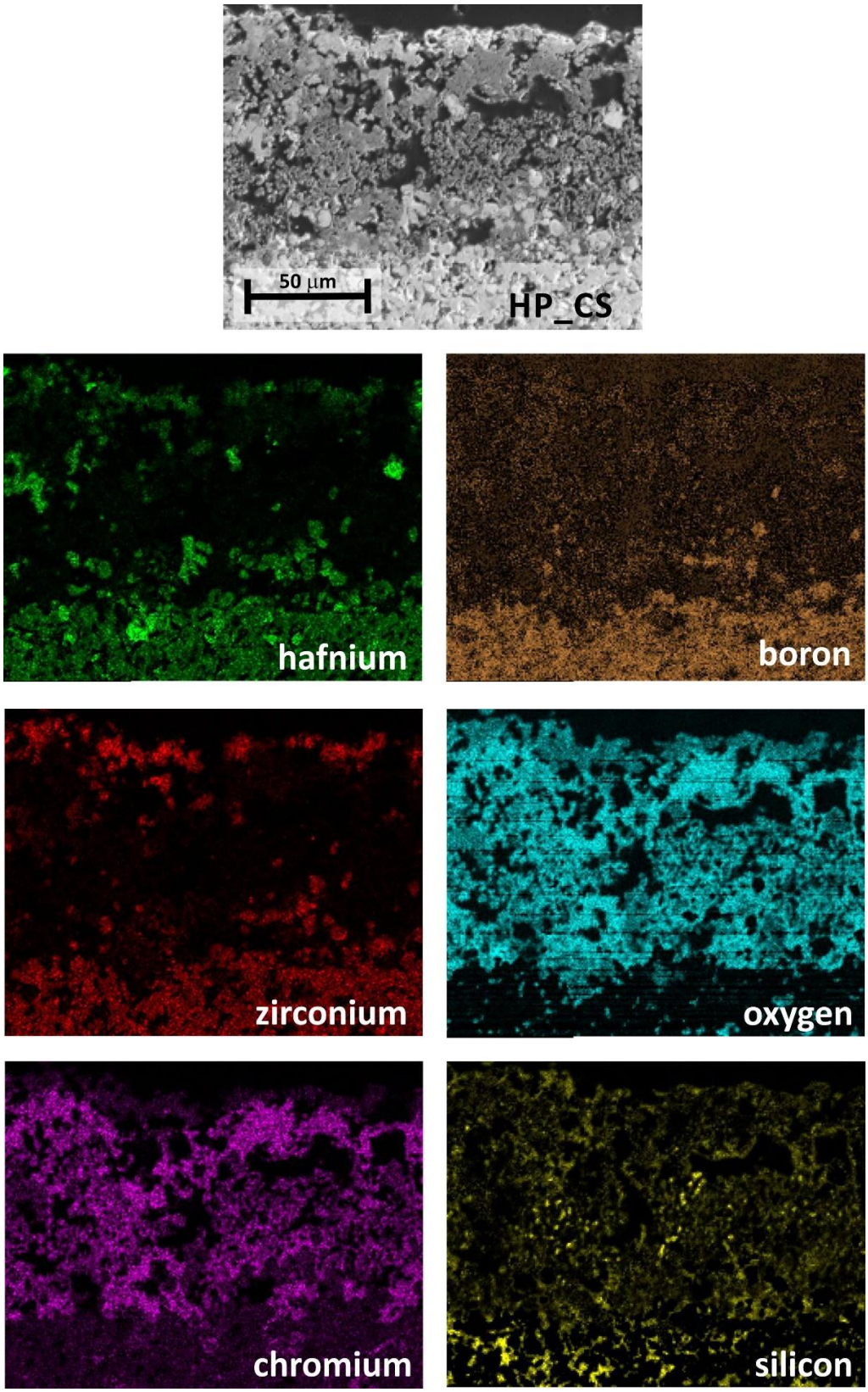


Figure S11. Elemental distribution maps along the oxidation profile in the HP_CS composite.